RESEARCH ARTICLE

Box-Behnken Design for Nephrolithiasis: Developing Folic Acid-Chitosan Nanoparticles from *Musa acuminata* Stem Water

Dessai P*, Pednekar P, Pednekar R

Department of Chemistry, Dnyanprassarak Mandal's College and Research Centre, Assagao, Bardez, Goa, India.

Received: 20th December, 2023; Revised: 16th February, 2024; Accepted: 30th June, 2024; Available Online: 31st August, 2024

ABSTRACT

Nephrolithiasis, or kidney stones, is a widespread condition causing significant discomfort and health issues. This analysis delves into the development of folic acid-chitosan nanoparticles (FA-CNPs) using *Musa acuminata* stem water to address nephrolithiasis. A Box-Behnken design was used to refine synthesis variables—chitosan concentration, folic acid loading, and reaction time. The study systematically analyzed their effects on nanoparticle size, encapsulation efficiency, and release profile. The optimized FA-CNPs demonstrated potential for improved targeted treatment of kidney stones, highlighting advancements in nanomedicine for effective nephrolithiasis management.

Keywords: Biocompatibility, Antioxidant, Kidney, nutrients, Nanoparticles.

International Journal of Pharmaceutical Quality Assurance (2024); DOI: 10.25258/ijpqa.15.3.20

How to cite this article: Dessai P, Pednekar P, Pednekar R. Box-Behnken Design for Nephrolithiasis: Developing Folic Acid-Chitosan Nanoparticles from *Musa acuminata* Stem Water. International Journal of Pharmaceutical Quality Assurance. 2024;15(3):1226-1231.

Source of support: Nil.

Conflict of interest: None

INTRODUCTION

Nanoparticles enhance drug delivery and bioavailability due to their size-dependent properties. Folic acid, crucial for cellular growth and repair, can be paired with chitosan to create targeted nanoparticles for treating kidney stones. *Musa acuminata* stem water, rich in bioactive compounds, serves as an eco-friendly material for nanoparticle synthesis.[1,2] Using Box-Behnken Design (BBD) allows for efficient optimization of synthesis conditions, improving the formulation and performance of folic acid-chitosan nanoparticles. This approach aims to enhance the therapeutic efficacy and stability of nanoparticles, advancing treatment strategies for nephrolithiasis.[3,4]

MATERIALS AND METHODS

Banana stems from Assonora Bardez in North Goa were collected post-ripening. Three factors at three levels were selected and encoded for analysis. Using Box-Behnken Design, 15 experimental batches were prepared and data was collected. *M. acuminata* stems were sliced into 1 to 2 mm pieces, refluxed with distilled water for 2 hours, filtered, and the pale-yellow extract was kept at 2 to 4°C for later use..[5,6]

Conjugation of Folic Acid with Chitosan

A 1:1 FA and triethylamine (TEA) solution in anhydrous dimethyl sulfoxide (DMSO) was combined with a 0.5% chitosan solution in 0.1 M acetic acid (pH 4.7) and stirred in the dark at 25°C for 16 hours. After adjusting the pH to 9.0 with 1 M NaOH, the mixture was centrifuged at 2500 rpm to precipitate the FA-CS conjugate. The precipitate was dialyzed in phosphate buffer (pH 7.4) for 3 days and water for 4 days, then freeze-dried and stored. [7,8]

Preparation of Nanoparticles (NPs)

Combining a 1:1 FA and triethylamine solution in anhydrous DMSO with a 0.5% chitosan solution in 0.1 M acetic acid (pH 4.7), the mixture was stirred at 25°C in the dark for 16 hours. After raising the pH to 9.0 with 1 M NaOH, it was centrifuged at 2500 rpm to precipitate the FA-CS conjugate. The precipitate underwent dialysis in phosphate buffer (pH 7.4) for 3 days, then water for 4 days, before being freeze-dried and stored. [9,10]

Biosynthesis of Nanoparticles

The banana stem water extract was combined with the folic acid-chitosan conjugation solution and stirred at room temperature for 1-hour. A color change indicated nanoparticle formation.[11,12]

Characterization of Nanoparticles

Fourier transform infrared spectroscopy (FTIR)

Using a Thermo Scientific Nicolet iS5 FTIR Spectrophotometer, the IR spectrum of the compound was recorded from 400 to 4000 cm^{-1} to identify functional groups in the nanoparticles.

*Author for Correspondence: desaiprabhat@yahoo.com

The nanoparticles were analyzed between KBr discs to determine the chemical structure of the folic acid-chitosan conjugate.[13,14]

Scanning electron microscopy (SEM)

A scanning electron microscope (SEM) employs a focused electron beam to produce detailed, high-resolution images of an object's surface, revealing its composition and physical features.[15,16]

Optimization: Box-behnken design

Three factors at three levels were selected from pre-tests and coded. The Box-Behnken model with three central points was used to randomly select and analyze 15 experimental batches.[17]

Optimization: Data analysis and validation

Pre-tests determined three factors at three levels, which were coded. The Box-Behnken model, including three central points, directed the selection and data collection from 15 experimental batches.[18]

Evaluation Studies of Nanoparticles

Invitro studies (For nephrothialiasis)

The kidney stone was weighed using a digital balance and placed in a semi-permeable cotton pouch. This pouch was suspended in a beaker containing 200 mL of filtered liquid extract, with the beaker covered and the pouch's lower end dipped in the liquid. The setup was placed on a magnetic stirrer at 200 rpm for 2 hours at room temperature. The liquid extract was replaced every 4 days, and the weight change of the stone was recorded. [19,20]

Antimicrobial activity of nanoparticles

- *Paper disk method*

The antimicrobial activity of nanoparticle solutions was assessed against *Staphylococcus aureus* and *Escherichia coli* using the paper disk method. Plant extract served as a negative control, and ampicillin (0.1 mg/mL) was the positive control. Inhibition zones were measured in mm after incubating the disks at 37°C for 24 hours.[21,22]

Antioxidant activity

Table 1: Lists of independent variables

Factor	*Parameter*	*Unit*	*Minimum value*	*Maximum value*
A	Polymer	mg	300	1200
B	Sonication time	min	15	60
C	Sonication frequency	KHz	20	60

Table 2: Lists of dependent variables

Response	*Name*	*Units*
R1	Entrapment Efficiency	%
R2	Practical Yield	%

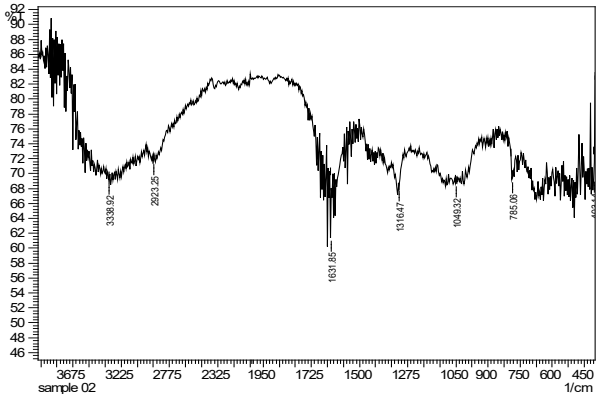

Figure 1: IR spectra of folic acid chitosan conjugate

Table 3: Interpretation of IR spectra

Functional group	*Expected values*	*Observed value*
R-CONH$_2$	1690–1630 cm^{-1}	1631.85 cm^{-1}
O-H (ACIDIC)	3300–2500 cm^{-1}	2923.25 cm^{-1}
N-H (BOND STRETCH)	3600–3200 cm^{-1}	3338.92 cm^{-1}

Table 4: Information of nanoparticles

Compound	*Morphology*	*Particle size*
Nanoparticles	Irregular shape in cluster	80–95 nm

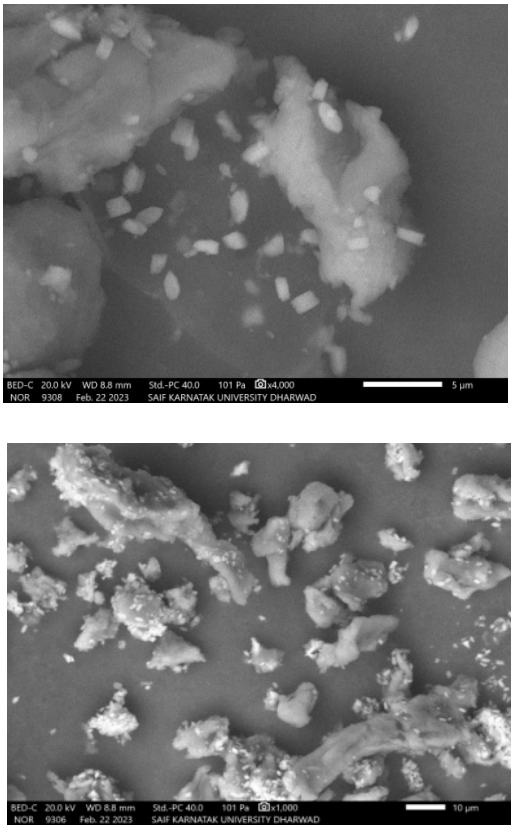

Figure 2: SEM images of nanoparticles

Table 5: Experimental Design: 15 Runs and Responses

Std	*Run*	*Factor 1: A: Polymer (mg)*	*Factor 2: B: Sonication time (min)*	*Factor 3: C: Sonication frequency (KHz)*	*Response 1: Entrapment efficiency (%)*	*Response 2: Practical yield (%)*
5	1	300	37.5	20	86.04	78.54
14	2	750	37.5	40	84.22	87.45
13	3	750	37.5	40	86.06	84.43
3	4	300	60	40	78.62	83.23
2	5	1200	15	40	89.48	78.02
12	6	750	60	60	86.34	87.93
6	7	1200	37.5	20	72.64	83.04
7	8	300	37.5	60	80.64	74.54
8	9	1200	37.5	60	82.64	89.4
15	10	750	37.5	40	86.04	84.54
1	11	300	15	40	76.76	78.54
9	12	750	15	20	83.64	89.43
4	13	1200	60	40	79.98	76.5
10	14	750	60	20	85.65	89.45
11	15	750	15	60	80.54	88.65

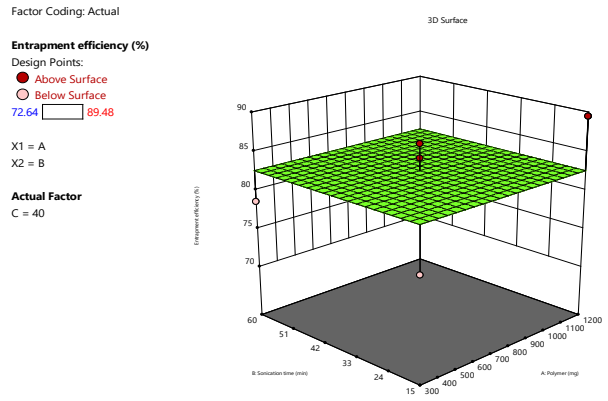

Figure 3: Counter plots of sonication time and polymer versus entrapment efficiency

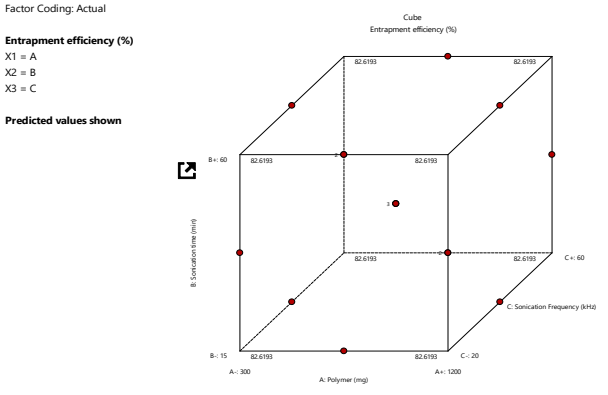

Figure 4: Cubic design illustrating the interaction between polymer, sonication time, and frequency on entrapment efficiency

Table 6: ANOVA analysis for entrapment efficiency

Source	*Sum of squares*	*Df*	*Mean square*	*F-value*	*p-value*	
Model	0.0000	0				
Residual	274.06	14	19.58			
Lack of Fit	271.83	12	22.65	20.29	0.0479	Significant
Pure error	2.23	2	1.12			
Cor total	274.06	14				

- *Hydrogen peroxide scavenging*

A 0.1 M H_2O_2 solution in phosphate buffer (pH 7.4) was prepared for the hydrogen peroxide scavenging assay. The extract was combined with 0.6 mL of this H_2O_2 solution in 3.4 mL of phosphate buffer, and the absorbance was measured at 230 nm.[23,24]

RESULTS AND DISCUSSION

Characterisation

FTIR analysis

Results are depicted in Figures 1 and Table 3.

Sem analysis

SEM analysis revealed that the nanoparticles have an irregular, clustered shape with a size range of 80 to 95 nm.

Optimization process variales of nanoparticle

Results are depicted in Table 5.

Table 7: ANOVA analysis for practical yield

Source	*Sum of squares*	*Df*	*Mean square*	*F-value*	*p-value*	
Model	211.07	2	105.54	7.60	0.0074	Significant
A-Polymer	18.33	1	18.33	1.32	0.2731	
A^2	192.74	1	192.74	13.87	0.0029	
Residual	166.71	12	13.89			
Lack of fit	160.84	10	16.08	5.48	0.1640	Not significant
Pure error	5.87	2	2.93			
Cor total	377.78	14				

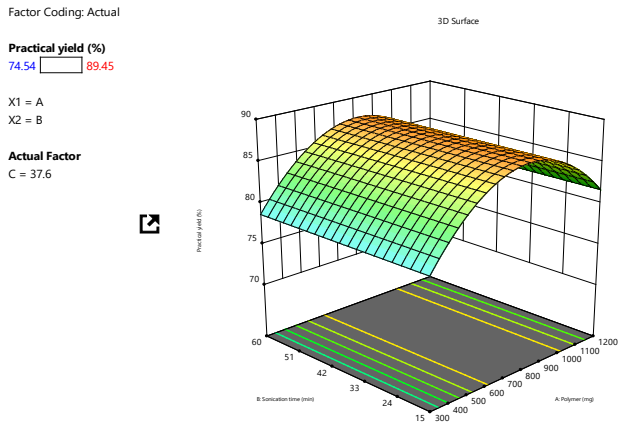

Figure 5: Counter plots of sonication time and polymer *versus* practical yield

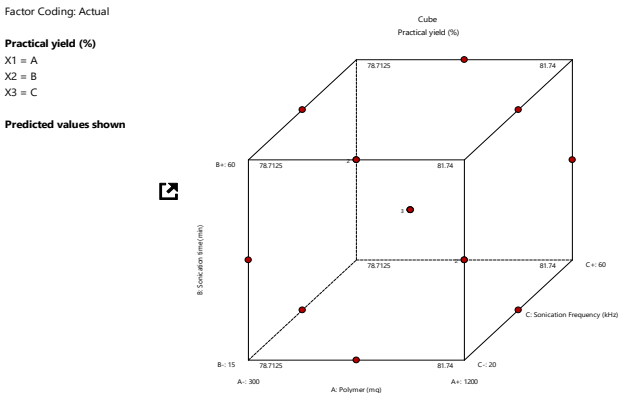

Figure 6: Impact of polymer type, sonication time, and frequency on entrapment efficiency in cubic design

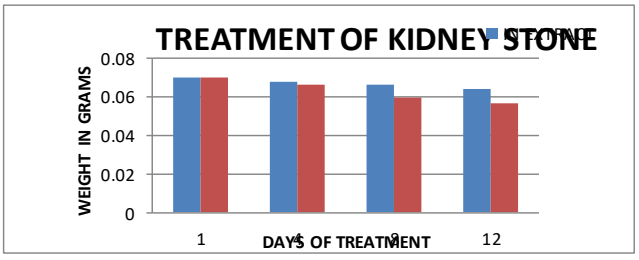

Figure 7: Comparison of stone weight in extract and nanoparticles

Anova for Mean Model

Response 1: Entrapment efficiency

Results are depicted in Table 6.

Factor coding is Actual

Sum of squares is type III - partial

In this case, no model terms are significant, as *p-value* are all above 0.0500. Terms with *p-value* above 0.1000 are deemed insignificant and may necessitate model reduction. Additionally, a Lack of Fit F-value of 20.29, with a 4.79% chance of occurring randomly, highlights a significant lack of fit, which is not ideal for achieving a good model.

ANOVA for Reduced Quadratic mode

Response 2: Practical yield

Results are depicted in Table 7.

Factor Coding is Coded

Sum of squares is type III - Partial

With a Model F-value of 7.60, there is only a 0.74% chance of obtaining such a large value by chance, indicating the model is significant. Significant model terms, including A^2, are identified by *p-value* below 0.0500, while terms with values above 0.1000 are not significant and may require model reduction. The Lack of Fit F-value of 5.48, with a 16.40% chance of occurring by chance, is not significant relative to pure error, suggesting the model fits well.

By performing optimization, 9 solutions were obtained out of which one was used for preparation.

Optimization, Validation and Evaluation

Design Expert recorded and analyzed optimized formulations (Table 9) using a mathematical model. The formulation with the best process conditions and desirability factors was selected. Under these optimized conditions, the solutions and nanoparticles were prepared. The prepared nanoparticles were compared with the plant extract. SEM analysis was performed to assess particle size and morphology. *In-vitro* studies for nephrolithiasis and comparative evaluations between nanoparticles and plant extract were conducted.

Evaluation of *in-vitro* studies (for nephrothialiasis)

Results are depicted in Table 9 and Figure 7.

Antimicrobial Activity

No zone of inhibition was observed for plant extract or nanoparticles against *E. coli* and *S. aureus.*

Only the positive control exhibited antimicrobial activity; neither *E. coli* nor *S. aureus* showed any inhibition zones for the nanoparticles or plant extract.

Antioxidant Activity

Antioxidant activity of the extract and nanoparticles was assessed *via* H_2O_2 scavenging at 230 nm.

From the above result, nanoparticles show more antioxidant activity than the extract.

Table 8: Solutions for optimum formulations

Number	*Polymer*	*Sonication time*	*Sonication frequency*	*Entrapment efficiency*	*Practical yield*	*Desirability*	*Remark*
1	300.000	37.500	40.000	82.619	77.017	1.000	Selected
2	750.000	37.500	40.000	82.619	85.473	1.000	
3	1200.000	37.500	40.000	82.619	80.044	1.000	
4	759.239	37.500	40.000	82.619	85.501	1.000	
5	456.636	37.500	40.000	82.619	81.536	1.000	
6	874.474	37.500	40.000	82.619	85.361	1.000	
7	736.279	37.500	40.000	82.619	85.421	1.000	
8	1173.314	37.500	40.000	82.619	80.753	1.000	
9	1084.016	37.500	40.000	82.619	82.772	1.000	

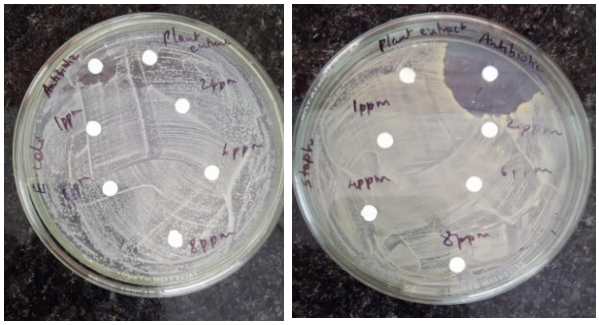

Figure 8: Inoculated agar plates of *E. coli* and *S. aureus*

Table 9: Comparison of stone weight in extract and nanoparticles

Days of treatment	*Stone weight in grams*	
	In extract	*In nanoparticles*
1	0.070	0.070
4	0.068	0.066
8	0.066	0.060
12	0.064	0.057

Table 10: Antimicrobial activities

Culture	*Zone of inhibition (nm)*	
	Extract	*Nanoparticles*
E. coli	-	-
S. aureus	-	-

Table 11: Antioxidant activity of extract

Tube	*Absorbance At 230 nm*	*% of antioxidant*
Control	0.972	-
Extract	0.550	43.415

Table 12: Antioxidant Activity of Nanoparticle

Tube	*Absorbance At 230 nm*	*% of antioxidant*
Control	1.092	-
Nanoparticle	0.461	57.783

SUMMARY

Addressing kidney stone recurrence, this study developed nanoparticles by conjugating folic acid with chitosan and reacting them with *M. acuminata* stem extract. FTIR confirmed amide bond formation, while SEM revealed irregular, clustered nanoparticles of 80 to 100 nm. Optimization via Box-Behnken Design improved production efficiency, resulting in nanoparticles with a mean diameter of 80 to 90 nm. In vitro tests showed these nanoparticles were more effective in dissolving kidney stones than the plant extract. Both showed no antimicrobial activity, but the nanoparticles had superior antioxidant activity

REFERENCES

1. Kuchekar A, Pawar S. Development and Evaluation of Luliconazole Loaded Nanoemulgel Using Box Behnken Design. 1. International Journal of Pharmaceutical Quality Assurance. 2024;15(2):616-621.
2. Sani YN, Haque M, Suryati K, Mohd KW, Khan A. Isolation and characterisation of andrographolide from *Andrographis paniculata* (Burm. F) wall. Ex nees and its total flavonoid effects from Kemaman, Malaysia. Int. J. Pharm. Qual. Assur. 2017;8(3):119-24.
3. Kujur A, Daharwal SJ. Box–Behnken Design-Based Optimization of Process Variables for the Green Synthesis of 18-Beta–Glycyrrhetinic Acid Silver Nanoparticles and Evaluation of Its Antioxidant, Antimicrobial Activity. Int. J. Drug Deliv. Technol. 2023;13(2):501-9.
4. Challa TR, Reshma K. Experimental design statistically by design expert software: A model poorly soluble drug with dissolution enhancement and optimization. International Journal of Drug Delivery Technology. 2022;12(3):1367-75.
5. Naghibi Beidokhti HR, Ghaffarzadegan R, Mirzakhanlouei S, Ghazizadeh L, Dorkoosh FA. Preparation, characterization, and optimization of folic acid-chitosan-methotrexate core-shell nanoparticles by box-behnken design for tumor-targeted drug delivery. Aaps Pharmscitech. 2017 Jan;18:115-29.
6. Doan VD, Le VT, Phan TL, Nguyen TL, Nguyen TD. Waste banana stem utilized for biosynthesis of silver and gold nanoparticles and their antibacterial and catalytic properties. Journal of Cluster Science. 2021 Nov;32:1673-82.
7. Venugopal V, Kumar KJ, Muralidharan S, Parasuraman S, Raj PV, Kumar KV. Optimization and *in-vivo* evaluation of isradipine

nanoparticles using Box-Behnken design surface response methodology. OpenNano. 2016 Jan 1;1:1-5.
8. Alelign T, Petros B. Kidney stone disease: an update on current concepts. Advances in urology. 2018;2018.
9. Ullah S, Azad AK, Nawaz A, Shah KU, Iqbal M, Albadrani GM, Al-Joufi FA, Sayed AA, Abdel-Daim MM. 5-fluorouracil-loaded folic-acid-fabricated chitosan nanoparticles for site-targeted drug delivery cargo. Polymers. 2022 May 13;14(10):2010.
10. Karmoker JR, Hasan I, Ahmed N, Saifuddin M, Reza MS. Development and optimization of acyclovir loaded mucoadhesive microspheres by box–Behnken design. Dhaka University Journal of Pharmaceutical Sciences. 2019 Apr;18(1):1-2.
11. Naghibi Beidokhti HR, Ghaffarzadegan R, Mirzakhanlouei S, Ghazizadeh L, Dorkoosh FA. Preparation, characterization, and optimization of folic acid-chitosan-methotrexate core-shell nanoparticles by box-Behnken design for tumor-targeted drug delivery. Aaps Pharmscitech. 2017 Jan;18:115-29.
12. Chen J, Huang L, Lai H, Lu C, Fang M, Zhang Q, Luo X. Methotrexate-loaded PEGylated chitosan nanoparticles: synthesis, characterization, and in vitro and in vivo antitumoral activity. Molecular pharmaceutics. 2014 Jul 7;11(7):2213-23.
13. Zhang C, Zhang Z, Zhao L. Folate-decorated poly (3-hydroxybutyrate-co-3-hydroxyoctanoate) nanoparticles for targeting delivery: optimization and in vivo antitumor activity. Drug delivery. 2016 Jun 12;23(5):1830-7.
14. Zhao P, Wang H, Yu M, Liao Z, Wang X, Zhang F, Ji W, Wu B, Han J, Zhang H, Wang H. Paclitaxel loaded folic acid targeted nanoparticles of mixed lipid-shell and polymer-core: in vitro and in vivo evaluation. European journal of pharmaceutics and biopharmaceutics. 2012 Jun 1;81(2):248-56.
15. Bagre AP, Jain K, Jain NK. Alginate coated chitosan core-shell nanoparticles for oral delivery of enoxaparin: in vitro and in vivo assessment. International journal of pharmaceutics. 2013 Nov 1;456(1):31-40.
16. Gajra B, Patel RR, Dalwadi C. Formulation, optimization and characterization of cationic polymeric nanoparticles of mast cell stabilizing agent using the Box–Behnken experimental design. Drug development and industrial pharmacy. 2016 May 3;42(5):747-57.
17. Adena SK, Upadhyay M, Vardhan H, Mishra B. Development, optimization, and in vitro characterization of dasatinib-loaded PEG functionalized chitosan capped gold nanoparticles using Box–Behnken experimental design. Drug development and industrial pharmacy. 2018 Mar 4;44(3):493-501.
18. Brar V, Kaur G. Preparation of chitosan okra nanoparticles: optimization and evaluation as Mucoadhesive drug delivery system. Pharmaceutical Nanotechnology. 2018 Sep 1;6(3):180-91.
19. Pawar H, Douroumis D, Boateng JS. Preparation and optimization of PMAA–chitosan–PEG nanoparticles for oral drug delivery. Colloids and Surfaces B: Biointerfaces. 2012 Feb 1;90:102-8.
20. Vozza G, Danish M, Byrne HJ, Frías JM, Ryan SM. Application of Box-Behnken experimental design for the formulation and optimisation of selenomethionine-loaded chitosan nanoparticles coated with zein for oral delivery. International journal of pharmaceutics. 2018 Nov 15;551(1-2):257-69.
21. Wang F, Wang Y, Ma Q, Cao Y, Yu B. Development and characterization of folic acid-conjugated chitosan nanoparticles for targeted and controlled delivery of gemcitabinein lung cancer therapeutics. Artificial cells, nanomedicine, and biotechnology. 2017 Nov 17;45(8):1530-8.
22. Li P, Wang Y, Zeng F, Chen L, Peng Z, Kong LX. Synthesis and characterization of folate conjugated chitosan and cellular uptake of its nanoparticles in HT-29 cells. Carbohydrate research. 2011 May 1;346(6):801-6.
23. Rohilla R, Garg T, Bariwal J, Goyal AK, Rath G. Development, optimization and characterization of glycyrrhetinic acid–chitosan nanoparticles of atorvastatin for liver targeting. Drug delivery. 2016 Sep 1;23(7):2290-7.
24. Jeevitha D, Amarnath K. Chitosan/PLA nanoparticles as a novel carrier for the delivery of anthraquinone: Synthesis, characterization and in vitro cytotoxicity evaluation. Colloids and Surfaces B: Biointerfaces. 2013 Jan 1;101:126-34.